NASA TECHNICAL MEMORANDUM

NASA TM X-52056

EFFECT ON SURFACE THERMAL PROPERTIES OF CALIBRATED EXPOSURE TO MICROMETEOROID ENVIRONMENT

by Herman Mark, Ralph D. Sommers, and Michael J. Mirtich
Lewis Research Center
Cleveland, Ohio

TECHNICAL PREPRINT prepared for Second
Aerospace Sciences Meeting sponsored by the
American Institute of Aeronautics and Astronautics
New York, New York, January 25-27, 1965

NATIONAL AERONAUTICS AND SPACE ADMINISTRATION · WASHINGTON, D.C. · 1964

[redacted]

EFFECT ON SURFACE THERMAL PROPERTIES OF CALIBRATED EXPOSURE TO MICROMETEOROID ENVIRONMENT

by Herman Mark, Ralph D. Sommers, and Michael J. Mirtich
Lewis Research Center
Cleveland, Ohio

TECHNICAL PREPRINT prepared for

Second Aerospace Sciences Meeting
sponsored by the American Institute of
Aeronautics and Astronautics
New York, New York, January 25-27, 1965

NATIONAL AERONAUTICS AND SPACE ADMINISTRATION

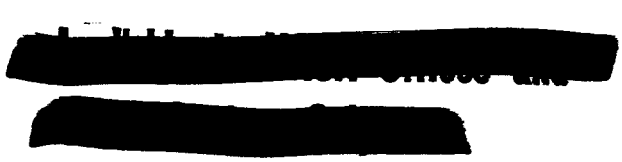

EFFECT ON SURFACE THERMAL PROPERTIES OF CALIBRATED EXPOSURE TO MICROMETEOROID ENVIRONMENT

by Herman Mark, Ralph D. Sommers, and Michael J. Mirtich

Lewis Research Center

29421

ABSTRACT

An accurate procedure for reproducing the exposure of metal surfaces to impaction by micron-size particles at hypervelocities has been employed to expose targets of several materials. After degradation of surface optical properties in varying amounts due to such exposure, these targets were mounted on a simulated space vehicle that was then placed in a solar-space-environment chamber. In this chamber the pressure was maintained below 10^{-13} mm Hg, the black radiation sink of space was provided at 4.2° K, and the samples were placed in a beam-simulating solar radiation. The intensity of the beam was maintained at 1 solar constant, while reproducing reasonably well the spectral distribution of solar radiation in space. Values of normal solar absorptance, total hemispheric emittance, and equilibrium temperature for various materials were thus obtained as a function of exposure to simulated micrometeoroid impaction. Comparison of these data with actual satellite sample temperature histories will allow an alternate method of estimating micrometeoroid flux in space, without the limitations of momentum calibrated microphone data, or the need for hard-to-interpret penetration flux measurements. author

INTRODUCTION

As part of an overall effort to determine the degradation of material surface properties while these surfaces are exposed to the micrometeoroid environment in Earth orbit, a program is in progress at the Lewis Research Center to simulate this environment. Since laboratory acceleration of projectiles to

meteoric speeds, while maintaining the projectile intact, has not been successfully accomplished as yet, it was the aim of this program to produce quantitatively the surface damage caused by collision with such particles over a range of the highest particle speeds presently attainable. From the surface damage at these speeds it was expected that extrapolation to the damage caused by microparticles impacting at meteoric speeds could be made, and thus remove the need for subjecting every material whose surface properties are of interest to actual space flight exposure.

A procedure for simulating the phenomena associated with micrometeoroid exposure has been developed and is described in reference 1. This procedure has made possible the quantitative exposure of various surfaces to impact by clouds of high-speed micron-size particles. This has subsequently allowed correlation of the change in optical properties (infrared reflectance or emittance) of various materials with the laboratory exposure, and thereby suggested the program that is the subject of the present paper.

This program consists of measuring the "in-space" temperature of thermally isolated disks that have been exposed to increasing amounts of simulated micrometeoroid environment. Transient as well as equilibrium measurements are included. The "space" is the working section of a large solar space-environment-simulation chamber in which the "in-space" thermal environment for the disks has been accurately reproduced. In this way a relation is obtained between the temperature histories of the disks and the amount of micrometeoroid exposure. At the same time an accurate picture of the surface damage associated with this exposure and hence with the temperatures is available, since the disks are in hand and can be examined by the appropriate optical instruments.

It would be most interesting to know the actual temperature history of the disk in space for comparison. Such a temperature history, together with the

temperature-exposure relation for a similar disk obtained in the present experiment on the ground, constitutes another method for estimating the exposure to micrometeoroid flux. This flux estimate is based on the change in optical properties of the exposed surfaces and the associated change in the temperatures of the disks, precalibrated by the laboratory exposure and space-simulator-temperature study herein described. In the present study this exposure-temperature "calibration" has been made for three materials, and these are presented along with a complete before-and-after-exposure optical description of the surfaces. Although a comparison with an actual space experiment is not made here, the expected temperature behavior of the "exposed" surfaces in space, and possible explanations and consequences of this behavior are presented.

SIMULATION OF MICROMETEOROID EXPOSURE

In spite of the fact that maximum attainable speeds to which particles could be accelerated intact were only a fraction of the speeds of encounter with the particles in Earth orbit, it was felt that the phenomenon of hypervelocity impaction with micrometeoroids could best be simulated by impaction with particles at attainable speeds, although other means of causing damage to surfaces have been suggested. In order to obtain a calibration of micrometeoroid exposure against equilibrium temperature of a thermally isolated disk under space conditions, a means of characterizing the exposure on the ground and in space was needed. Both the laboratory exposure and the change in surface property (reflectance, for instance) due to the exposure are known on the ground, but it is clear that the change in surface property could have been caused in a number of ways, and thus, not having a unique tie to the environment that caused it, fails to characterize this environment as well as the exposure itself. Therefore, the question remains as to the actual physical quantity to use for measuring the exposure. Since a number of earlier investigations, experimental as

well as theoretical, have indicated that the volume of the craters formed in targets as a result of impaction with high-speed projectiles is proportional to the kinetic energy of the projectiles, the sum of the kinetic energies of the particles striking the surface up to any time was chosen as the physical quantity characterizing the exposure. The analysis that follows from this is presented in references 1 and 2 and provides a useful relation connecting the surface reflectance with the exposure characterized by the kinetic energy of the particles impacting. From reference 1, the expression for reflectance $\bar{\rho}_a$ of a metal surface of area A_o exposed to impaction by particles having a total kinetic energy $\mathcal{E}$ in joules is

$$\bar{\rho}_a = \bar{\rho}_i \left[1 - \left(1 - \frac{\bar{\rho}_\infty}{\bar{\rho}_i} \right) \left(1 - e^{-K_1 \mathcal{E}} \right) \right] \tag{1}$$

where

$$K_1 = \frac{2}{A_o} \left(\frac{3\pi^{1/2}}{4E_{cr}} \right)^{2/3} \left(m_p v_p^2 \right)^{-1/3} \tag{2}$$

All symbols are defined in appendix A.

Equations (1) and (2) allow an analytical extrapolation from the measured total energy required for a given laboratory-caused surface optical property change, to the total energy required in space for the same surface optical property change. This extrapolation requires evaluating K_1 for space and can be done if the kinetic energy of the particle in space causing most of the surface damage can be reasonably estimated (see appendix B).

The experimental procedure for producing the laboratory damage to the surfaces is described in detail in reference 1, but, briefly, quantitative exposures were obtained in the following way.

Polished surfaces of soft aluminum, stainless steel, and stainless steel coated with 1900 angstroms of aluminum were bombarded by clouds of SiC particles

having an average diameter of 6 microns and a speed of 8500 feet per second. The particles were accelerated by the aerodynamic drag of the short duration flows in a shock tube and the resultant kinetic energies

$$\mathcal{E} = \sum_{i=1}^{N} \frac{1}{2} m_{p_i} v_{p_i}^2 \tag{3}$$

were obtained from strip-film camera measurements for particle speed, and microbalance collection measurements to determine the total number of particles striking the given area (see ref. 1). The measurement of speed and number of particles striking a plate were quite accurately reproducible, and the laboratory exposures were measured and are presented in joules. In each series (i.e., for each target material) the disks were nominally exposed to 0, 1, 2, 4, and 6 joules. This range of exposures represents changes in the reflectance of a single disk from its original value near 1.0 to about 0.5.

Thus, there is the possibility of quantitatively exposing surfaces in the laboratory to impaction by high-speed particles (energy measured in joules), measuring the damage (change in surface optical properties) with a spectrometer and then, from analytical considerations using equations (1) and (2), calculating the equivalent space exposure (again in joules) required to produce the same surface damage. Having the space exposure-surface damage relation, plus the surface damage-equilibrium temperature relation obtained in the simulated space environment (described in a later section), allows the simple monitoring of the temperature of a disk in space to determine not only the surface damage but also the actual micrometeoroid exposure causing the damage as a function of time. This follows, of course, only if it is assumed that only the micrometeoroid exposure is causing the surface damage. This is probably true, in space, for many of the important materials whose surfaces will be exposed. It is also necessary

to assume that normal impingement is sufficient to simulate impingement from all directions. This is shown to be so and is discussed in reference 3.

DETERMINATION OF SURFACE OPTICAL PROPERTIES

The disks of the present study chosen for their good reflective properties were stainless steel, aluminum, and a stainless-steel substrate with a vacuum-deposited coating of aluminum 1900 angstroms thick. This coating is sufficiently thick for the surface to exhibit the optical properties of aluminum as long as the coating remains undamaged. Thus, we have built into the experiment a check on the life of a 1900 angstroms aluminum coating on stainless steel, for, presumably, when the coating has been eroded away, the substrate surface should again exhibit the properties of the exposed stainless steel.

The disks were chosen 15/16-inch in diameter and 1/64- to 1/16-inch thick, essentially because these are appropriate dimensions for a sample in the heated-cavity spectrometer system for making reflectance measurements. In this system a Perkin-Elmer 13U spectrometer compares, in a given wavelength band, the radiation from a blackbody cavity at about 600° C with the total radiation reflected from a water-cooled sample in the same wavelength band. This technique is quite good in the infrared region but is not satisfactory at shorter wavelengths due to insufficient radiation from the heated cavity below a wavelength of about 1 micron. The intensity ratios obtained in this way (I_{refl}/I_{HR}) are plotted as a function of wavelength and are plotted as a function of wavelength and are presented for a representative sample of each material in figure 1 both before and after exposure to impaction with approximately 1 joule of 6-micron-diameter SiC particles traveling at 8500 feet per second. The average values of these spectral data are also presented. The average reflectance is defined here as the single value that will reflect the same amount of energy arriving from a 420° K (756° R) blackbody source as does the sample, that is, the average

reflectance is given by

$$\bar{\rho}_a = \frac{\int_{\lambda_1}^{\lambda_2} \rho_{h-a}(\lambda) I_{BB}(\lambda) d\lambda}{\int_{\lambda_1}^{\lambda_2} I_{BB}(\lambda) d\lambda} \qquad \lambda_1 = 1.5 \text{ microns}, \ \lambda_2 = 15.5 \text{ microns} \qquad (4)$$

where $\rho_{h-a} = I_{refl}/I_{HR}$.

The normal solar absorptance was determined from measurements made in the space environment simulator during transient heating of the exposed disks mounted in a simulated space vehicle (see appendix C). The total hemispheric emittance of the disks was obtained during transient cooling (see appendix C). Comparisons are made later between equilibrium temperatures calculated from the values of thermal optical properties obtained by these transient experiments and the actual equilibrium temperatures attained by the disks in the solar simulator. Infrared reflectances are also compared with thermally obtained disk emittances as a further check. The space chamber thermal experiment will be described in the next section.

TEMPERATURE HISTORIES OF EXPOSED DISKS IN SIMULATED SPACE ENVIRONMENT

Space Environment Facility

In order to study problems induced by the environment that a vehicle and its components will see in space, several facilities have been designed and built at the Lewis Research Center to reproduce this environment. The space-environment-simulation facility employed in the equilibrium temperature experiment of the present paper is the ultimate facility available at the present time for simulating the thermal environment of space and a cutaway drawing is presented in figure 2. In the working section of the inner "space" chamber, which is 6 feet in diameter and approximately 10 feet high, four characteristics of

the space environment are reproduced simultaneously, and as accurately as possible. The first of these is the extremely low pressure of the gases in space, estimated to be about 10^{-14} mm Hg (to reproduce particle fluxes). This low pressure is obtained by using the enormous gas removal capabilities of the entire chamber wall kept at liquid-helium temperatures by jacketing. Two other characteristics that are provided simultaneously by jacketing the inner space chamber walls with liquid helium are the extremely low background temperature of space at about 4° K (thus removing any superfluous radiation source) as well as the very nearly perfect absorption capability of the space background for gases and radiation energy that a blackened wall at this temperature exhibits. The most important energy source in solar space is, of course, the Sun, and in this facility the radiation arriving from the Sun, at Earth distance from the Sun (but outside Earth atmosphere) is provided at the proper intensity, uniformity, and collimation angle, as well as with a spectral energy distribution quite like that of the Sun over the wavelength range from 3500 angstroms to about 2.5 microns.

To produce the liquid helium necessary for jacketing the inner 6-foot-diameter chamber, a helium liquefaction plant is in operation that has a capacity of more than 200 liters of liquid helium an hour. This liquid is stored in two 7000-liter liquid-helium Dewars from which it is drawn during the experiment. The liquefaction system can also be operated in a refrigeration mode and when so operated provides sufficient gaseous helium to keep the inner space chamber wall at 18° K, with a 1000-watt heat load in the chamber. This is sufficient to remove the energy introduced into the chamber by the solar-radiation simulator, plus some additional heat loads from the test vehicle.

The solar-radiation simulator has been described in detail in reference 4. It consists of a cored-carbon-electrode high-current arc with the focusing and

collimating optics required to form the necessary beam. The beam is brought into an evacuated collimating-mirror-support tank through a small window. It then passes up toward the collimating mirror and again down through a quartz window into the space chamber and on to the test plane, as shown in figure 2.

The intensity of the beam is monitored during the experiment by silicon solar cells that have been calibrated against total intensity meters before the experiment and then mounted on a ring surrounding the test vehicle. For temperature measurements on the test vehicle, copper-constantan thermocouples are used, while gold-cobalt-copper thermocouples are used whenever temperatures below 80° K are encountered (as on the chamber wall). Pressure measurements are made by means of tubulated cold-cathode ionization gages located at various stations in the chamber and pointed in a variety of directions to permit an average of the directional effect.

Space-Chamber-Temperature Experiment

Five originally identical 15/16-inch-diameter polished disks were selected for a given material and each disk was then subjected to a given amount of laboratory exposure, the exposure increasing from disk to disk. The range of exposure for the disks was sufficient to represent a change in a single disk from its original high reflectance near 1 at zero exposure, to a reflectance of about 0.5 at the maximum exposure. Although it is not certain how much time in space such degradation requires, the exposure in joules was accurately measured in the laboratory and the surface optical properties of each exposed disk was accurately determined by a hohlraum-spectrometer measurement and recorded. The nominal amount of exposure for the five disks in the present experiment was 0, 1, 2, 4, and 6 joules, respectively. This schedule was adhered to for three series of disks of the materials mentioned earlier. For the aluminum disk, the last exposure was increased to 25 joules to see the effect of "infinite" exposure.

Each series of disks (a given disk material) was then mounted on a simulated vehicle that had been so designed as to minimize the heat transfer between the vehicle and the disks mounted on it (fig. 3). This was accomplished by mounting the disks on nonconducting plastic stems and shielding the back of the disks with highly reflecting cups, thus allowing a heat balance for the disks only involving received and emitted radiation from the front exposed side of the disk and a minimum loss from the unexposed side (3×10^{-12} Btu/(hr)($^{o}R^{4}$)). The simulated vehicle was so mounted in the space-environment tank that the front faces of the disks received solar radiation falling directly on them in a direction normal to their surface. This front surface of the disk could also see the cold sink of space over almost the entire 2π solid angle (except for the Sun). Thus, the disk could arrive at the equilibrium temperature based on the heat balance between the normal energy (solar radiation) absorbed and the total hemispheric energy emitted by the front face (plus the energy loss to the supporting vehicle, see appendix C). The equilibrium temperatures were measured for each disk by a copper-constantan thermocouple embedded in the disk one-half the radius out from the mounting pin at the center. The equilibrium temperature of the disk was determined by approaching equilibrium conditions from above and below the equilibrium temperature. The radiation intensities were monitored during the experiment by six silicon solar cells previously calibrated against a Schwarz total radiation intensity meter. The resultant variation of the equilibrium temperature for all the disks is the result of reproducible changes in surface optical properties caused by calibrated exposure to high-speed micron-size-particle impaction.

Transient temperatures were measured similarly but were determined during heating and cooling of the disks for the purpose of determining α_{SN} and e_{TH} by an essentially independent experiment (independent from the equilibrium

experiment). Automatic data recording equipment made readings at appropriately signaled time intervals, and the method of appendix C was employed for calculating these values of thermal optical properties.

RESULTS

Simulated Exposure and Surface Damage

Reflectances for all the disks were obtained both before and after exposure, and spectral reflectance data of the type presented in figure 1 were calculated from equation (4) to obtain average values weighted for the energy distribution corresponding to a 420° K (756° R) blackbody. In figure 4 are presented all the average reflectance ratios for stainless steel, aluminum, and aluminum on stainless-steel substrate samples, plotted against the total energy of laboratory exposure. For equal damage in space, we have also presented the required space exposure on two additional abscissas (see appendix B). The first is for a space particle of 3×10^{-11} gram or a mass of one-tenth of the laboratory particle, and a speed of 34,000 feet per second (compared with 8500 ft/sec for the laboratory speed). The second extra abscissa is also for a 3×10^{-11} gram particle but at 85,000 feet per second. In the former case there is required an exposure of $\mathscr{E}_{SP_1} = 1.17\ \mathscr{E}_L$. In the latter case, $\mathscr{E}_{SP_2} = 2.15\ \mathscr{E}_L$. This increase in exposure at space conditions to obtain equivalent damage is due to the negative one-third exponential dependency on the single particle kinetic energy of the K_1 in equations (1) and (2). Thus, as the single particle kinetic energy increases, K_1 decreases (eq. (2)), and the surface damage at a given total energy of exposure is reduced (i.e., the reflectance does not fall as rapidly with total exposure).

The data of figure 4 indicate that the reduction in infrared reflectance ratio of aluminum is somewhat greater at any exposure than is that of stainless steel. The reflectance of both, however, fall after only 7.5 joules of labo-

ratory exposure to less than 60 percent of their original value. The reflectance ratio of the disk of stainless steel coated with 1900 angstroms of aluminum follows the reflectance ratio of aluminum until the exposures are somewhat increased, and then the values draw away from the aluminum and approach those of the substrate stainless steel as the aluminum coating is being eroded away. To obtain these curves, the values for $\overline{\rho}_\infty$, the reflectances of the samples at "infinite" exposure, were determined but are not shown here. The value for aluminum (obtained at 25 joules exposure) was 0.3055. For stainless steel, $\overline{\rho}_\infty/\overline{\rho}_i = 0.350$ (obtained at 30 joules exposure). In addition to pointing out the reduction in exposed surface reflectivity, figure 4 also suggests that the aluminum-coated disk should degrade like aluminum at first, then after some exposure and as the coating is removed, resemble the degradation rate of the substrate stainless steel. Since the reflectance ratio degradation rate for the aluminum coated surface has slowed to that of the stainless steel, the effect of the aluminum coating on stainless steel is to keep the absolute reflectance up throughout our experiment longer than that of aluminum alone, and hence for a longer time than might be expected in space.

Space-Chamber-Temperature Experiment

The major results of the temperature-equilibrium experiment are presented in figure 5 and tables I and II. In figure 5 are presented the "history" of the equilibrium temperature for disks of three different materials mounted on a simulated space vehicle and "flown" in a simulated space environment at 1.25 solar constants. These equilibrium temperatures are shown as they vary with exposure to micrometeoroid environment, the exposure being expressed in joules of energy of the impacting hypervelocity particles. Perhaps the most important feature of these curves is that, in spite of the large exposure to impacting particles, the resultant large change in optical properties measured in the

laboratory and the efforts made to isolate the disk thermally from its support, the total variation in equilibrium temperature of the disks is small but measurable. For the aluminum disk the measured change in equilibrium temperature is approximately 38° R or about 5 percent in absolute temperature level. For stainless steel the temperature is almost constant, varying only about 1 percent in absolute temperature level. The largest variation with exposure was for the aluminum-coated stainless-steel disk which rose 91° R due to the exposure or about 12 percent in absolute temperature level. The equilibrium temperature variations as measured for the disks and presented in figure 5 are also presented in table I for comparison with the equilibrium temperature calculated for the disks by using values for α_{SN} and e_{TH} determined from the two auxiliary nonsteady experiments (the first Sun-on, the other Sun-off). The check obtained between measured and calculated values is quite good. Also presented in this table are these values of α_{SN} and e_{TH} measured in the thermal transient experiment for each of the disks as the laboratory exposure is increased. It is clear from this information that both α_{SN} and e_{TH} are rising due to the exposure. Both stainless steel and aluminum on stainless steel are leveling off to about the same temperature. This is perhaps expected, too, as the aluminum coating is worn from the stainless-steel substrate. The all-aluminum disk is wearing most rapidly and exhibits the strongest rise in e_{TH}, but not the highest α_{SN}, hence it approaches the lowest equilibrium temperature in figure 5.

For the information presented in table II the e_{TH} of table I was used to calculate a fictitious reflectance $(1 - e_{TH})$, solely for comparison with $\bar{\rho}_a$, the average reflectance of the disks measured by the spectrometer method (ρ_{h-a}). These two "reflectances" can be compared because $\bar{\rho}_a$ is approximately equal to ρ_{h-h}, for the materials of this experiment, and ρ_{h-h} can be taken

equal to $(1 - e_{TH})$ at the same temperature.* The comparisons of these two quantities for all the disks are amazingly good considering the difference in the paths traveled to obtain them. Whether or not such a comparison is strictly correct, the optical or thermal changes in surface property are certainly varying in a very similar manner with simulated exposure to micrometeoroid environment.

This similarity in the variation of reflectance with exposure as measured by either method suggests the possibility of making reflectance measurements in space without a reflectometer, and also suggests using these reflectance measurements to determine micrometeoroid flux. This could be done by calibrating the change in temperature of a disk in a space-environment-simulation chamber with the measured (elsewhere) optical change of the surface caused by calibrated exposure of the disk to simulated micrometeoroid flux. Telemetering the temperature of the disk from a space experiment would then give not only the change in reflectivity of the disk but also, from correlation with the ground experiment, the micrometeoroid flux causing this reflectivity change.

DISCUSSION OF RESULTS

The reduction in infrared reflectance shown spectrally in figure 1, and as reflectance ratio $\bar{\rho}_a/\bar{\rho}_i$ against exposure in figure 4 is satisfactorily pre-

*The spectrometer measures ρ_{h-a} by determining the energy reflected from the hemispherically-illuminated cooled sample into a small beam at 16° from the normal to the surface of the sample, and comparing this quantity with the energy in the same small solid angle leaving the blackbody cavity (hohlraum). This value, spectrally averaged by equation (4) gives $\bar{\rho}_a$. This is still only the value for reflection 16° from the surface normal but can be taken approximately equal to ρ_{h-h}, the hemispheric value, since the angular reflectance values for surfaces considered here vary at most about 10 percent overall.

dictable for quantitative laboratory exposures. The resulting optical properties after exposure are quite reproducible in the laboratory, and equation (1) with an appropriate value for K_1 and $\overline{\rho}_\infty$ is amazingly good in predicting these optical properties. However, since these laboratory exposures are made with particles traveling at one-tenth to one-fourth the speed estimated for micrometeoroid particles, it remains to be seen, in the laboratory and in space, if the dependence of K_1 on particle kinetic energy is correct (eq. (2)), and thus, by using equation (1) with a space value for K_1, allow similarly good estimates of surface degradation rates at space conditions. The laboratory verification of this dependence is now being sought at a 50 percent increase in exposure speed (13,000 ft/sec) in experiments to be performed. In any case, a conservative estimate of appendix B indicates that the total exposure for equal surface damage should only increase by a factor of 2 at space conditions. This indicates that meteoroid flux data uncertainties are still the major factor preventing good quantitative estimates of surface life in space. However, since our ability to predict surface damage for a given exposure is good, it is suggested that this relation be inverted to determine the exposure from the surface damage, that is, monitor the reflectance of a polished metal surface in space to determine the exposure.

The second part of the present experiment, in which the "space" temperatures of exposed disks were determined as a function of surface optical properties resulting from known exposure, is an attempt to determine the difficulty of making "reflectance" measurements in space without a reflectometer. The results indicate that equilibrium temperatures of surfaces exposed to micrometeoroid impaction may vary only a small amount even after considerable surface degradation. Hence, unfortunately, there are very stringent requirements on measuring and telemetering techniques for obtaining any exposure information from surface

equilibrium temperature measurements on a flight experiment. These requirements can be relaxed somewhat by precalibrating polished disks on the ground to determine what their equilibrium temperature histories should be (as in fig. 5), but it still appears that nonsteady temperatures must also be used to clarify the picture. If this is carefully done the condition of the surface can become very clear (tables I and II) and a good check obtained between thermal and optical information.

CONCLUDING REMARKS

As a result of a program in which polished metal surfaces are exposed to impaction by high-speed micron-size particles in the laboratory, a quantitative relation is available between exposure in joules and degradation of surface optical properties for several materials. A flight experiment could be used, then, to monitor surface optical properties (reflectance, for instance) and, inverting this relation, determine exposure to micrometeoroid flux. "Reflectance" measurements in flight without a reflectometer are possible, and can be made with thermal measurements only. They must be made very carefully, however, since the equilibrium temperatures of polished metal disks in a typical satellite configuration may vary only a small amount even after considerable surface degradation. Hence, useful information regarding degradation may be obtainable only with nonsteady temperature measurements in flight, combined with preflight ground calibration of temperature histories of the exposed surfaces under simulated space conditions. Information concerning reflectance degradation of solar collectors in space could be determined in this manner.

APPENDIX A

SYMBOLS

A_o area of disk

C_p specific heat of disk material

d thickness of disk

E_{cr} cratering energy density, ergs/cc

e_{TH} total hemispheric emittance

$\mathcal{E}$ exposure, $\sum_i \frac{1}{2} m_{p_i} v_i^2$, joules

I_{HR} intensity from blackbody cavity

I_{SB} spectral energy distribution of 420° K (756° R) blackbody

K net energy exchange coefficient from disk to mounting cup, Btu/(hr)($^oR^4$)

K_1 defined in eq. (2)

m_p mass of impacting particle

R disk radius

T_c cup temperature

T_d disk temperature

t time

v_p particle velocity

α_{SN} normal solar absorptance

λ wavelength of radiation, microns

$\overline{\rho}$ average reflectance

ρ_d density of disk material

$\rho_{h\text{-}a}$ hemispheric angular reflectance

$\rho_{h\text{-}h}$ hemispheric-hemispheric reflectance

σ Stefan-Boltzmann constant, 1.713×10^{-9} Btu/(hr)(sq ft)($^oR^4$)

φ intensity of incident radiation

Subscripts:

a after expsosure to $\mathcal{E}$

i initial value

L laboratory conditions

SP_1 space conditions 1 (see appendix B)

SP_2 space conditions 2 (see appendix B)

APPENDIX B

SPACE EXPOSURE FOR EQUAL DAMAGE

In equation (1) of this paper the surface reflectance after exposure to impaction $\mathcal{E}$ is written

$$\overline{\rho}_a = \overline{\rho}_i \left[1 - \left(1 - \frac{\overline{\rho}_\infty}{\overline{\rho}_i} \right) \left(1 - e^{-K_1 \mathcal{E}} \right) \right] \tag{B1}$$

where

$$K_1 = \frac{2}{A_o} \left(\frac{3\pi^{1/2}}{4E_{cr}} \right) \frac{1}{\left(m_p v_p^2 \right)^{1/3}} \tag{B2}$$

For equal damage on a given surface, that is, constant $\overline{\rho}_a$, the quantity $K_1 \mathcal{E}$ must be held constant. If K_1 changes with single particle kinetic energy as in equation (B2), $\mathcal{E}$ must change to keep

$$K_{1_L} \mathcal{E}_L = K_{1_{SP}} \mathcal{E}_{SP} \tag{B3}$$

or

$$\mathcal{E}_{SP} = \left(\frac{K_{1_L}}{K_{1_{SP}}} \right) \mathcal{E}_L \tag{B4}$$

from equation (B2)

$$K_1 \sim \left(m_p v_p^2 \right)^{-1/3}$$

and equation (B4) becomes

$$\mathcal{E}_{SP} = \left(\frac{m_{p_{SP}} v_{p_{SP}}^2}{m_{p_L} v_{p_L}^2} \right)^{1/3} \mathcal{E}_L \tag{B5}$$

Thus, for the higher particle kinetic energies in space the total exposure required for the same damage is increased.

In the laboratory exposure the particle mass was 3×10^{-10} gram. For space, a good estimate of the mass of the most numerous particle may be made by finding the leveling-off point of the cumulative flux curve from reference 5, which presents the compiled microphone data presently available. Our best figure for the most numerous (minimum size) particle in space from this data is about 3×10^{-11} gram, or one-tenth of the laboratory particle mass. Estimates for particle speed in space vary from 30,000 to 200,000 feet per second. To calculate several examples we have taken one at 34,000 feet per second (four times lab speed) and 85,000 feet per second (10 times lab speed). Using equation (B5) we have

Case 1:

Let

$$m_{p_{SP}} = \frac{m_{p_L}}{10}$$

and

$$v_{p_{SP}} = 4v_{p_L}$$

Then

$$\mathscr{E}_{SP_1} = \left[\left(\frac{m_{p_{SP}}}{m_{p_L}}\right)\left(\frac{v_{p_{SP}}}{v_{p_L}}\right)^2\right]^{1/3} \mathscr{E}_L$$

$$\mathscr{E}_{SP_1} = \left[\left(\frac{1}{10}\right)(4)^2\right]^{1/3} \mathscr{E}_L$$

$$\mathscr{E}_{SP_1} = 1.17\ \mathscr{E}_L$$

Case 2:

Let

$$m_{p_{SP}} = \frac{m_{p_L}}{10}$$

$$v_{p_{SP}} = 10\ v_{p_L}$$

$$\mathcal{E}_{SP_2} = \left[\left(\frac{1}{10}\right)(10)^2\right]^{1/3} \mathcal{E}_L$$

$$\mathcal{E}_{SP_2} = 2.15\ \mathcal{E}_L$$

APPENDIX C

DETERMINATION OF EFFECTIVE OPTICAL PROPERTIES AND EQUILIBRIUM TEMPERATURE LEVELS

A determination of the effective optical properties α_{SN} and e_{TH} was effected through the use of data obtained during nonsteady (heating and cooling) portions of the space chamber tests. The following equation was used to describe the energy exchange:

$$\alpha_{SN} = \frac{\sigma e_{TH} T_d^4}{\varphi} + \frac{K\left(T_d^4 - T_c^4\right)}{\varphi \pi R^2} + \frac{\rho C_p d}{\varphi} \frac{dT_d}{dt} \tag{C1}$$

Total hemispherical emittance was determined from data obtained during times of no solar irradiance ($\varphi = 0$) and equation (C1) in the form

$$e_{TH} = -\left[\frac{\rho C_p d \frac{dT_d}{dt}}{\sigma T_d^4} + \frac{K\left(T_d^4 - T_c^4\right)}{\sigma \pi R^2 T_d^4}\right] \tag{C2}$$

Normal solar absorptance was determined by using data obtained during periods of heating, the previously determined e_{TH}, and equation (C1).

An equilibrium temperature, utilizing the α_{SN} and e_{TH} values obtained during nonsteady portions of the test, can be calculated from equation (C1) in the form

$$T_{eq}^4 = \frac{\left(\alpha_{SN} + \frac{KT_c^4}{\varphi \pi R^2}\right)}{\left(\frac{\sigma e_{TH}}{\varphi} + \frac{K}{\varphi \pi R^2}\right)} \tag{C3}$$

Experimentally, the equilibrium temperatures were determined by approaching equilibrium conditions from values below and values above the equilibrium temperature. This procedure resulted in two asymptotic approaches to equilibrium that bracketed the actual equilibrium levels and allowed a ready determination of the equilibrium temperatures within 5° F.

The calculated and measured data are presented in table I.

REFERENCES

1. Mirtich, Michael J., and Mark, Herman: Alteration of Surface Optical Properties by High-Speed Micron Size Particles. NASA TM X-51337, 1964.

2. Mark, Herman, Goldberg, Gary, and Mirtich, Michael J.: Determination of Cratering Energy Densities for Metal Targets by Means of Reflectivity Measurements. AIAA Jour., vol. 2, no. 5, May 1964, pp. 965-966.

3. Summers, James L.: Investigation of High-Speed Impact: Regions of Impact and Impact at Oblique Angles. NASA TN D-94, 1959.

4. Uguccini, Orlando W., and Pollack, John L.: A Carbon-Arc Solar Simulator. Paper 62-WA-241, ASME, 1962.

5. Alexander, W. M., McCracken, C. W., Secretan, L., and Berg, O. E.: Review of Direct Measurements of Interplanetary Dust from Satellites and Probes. Space Res. III: Proc. Third Int. Space Sci. Symposium, Sec. C2, Paper I, W. Priester, ed., John Wiley & Sons, Inc., 1963, pp. 891-917.

TABLE I . - VARIATION OF OPTICAL PROPERTIES AND EQUILIBRIUM TEMPERATURES OF METAL DISKS WITH EXPOSURE

Aluminum					
Lab exposure, joules	0	1.25	2.68	5.6	25.4
α_{SN}	0.230	0.447	0.451	0.572	1.02
e_{TH}	0.061	0.184	0.243	0.282	0.675
$T_{eq(calc)}$, ^{o}F	270	311	290	315	317
$T_{eq(meas)}$, ^{o}F	265	295	287	303	305
304 Stainless steel					
Lab exposure, joules	0	0.909	2.16	4.26	6.49
α_{SN}	0.432	0.579	0.618	0.691	0.793
e_{TH}	0.112	0.221	0.301	0.338	0.366
$T_{eq(calc)}$, ^{o}F	338	337	319	326	350
$T_{eq(meas)}$, ^{o}F	328	338	329	330	336
Aluminum (1900 angstroms) on 304 stainless steel					
Lab exposure, joules	0	1.05	1.98	4.51	6.08
α_{SN}	0.111	0.428	0.475	0.563	0.702
e_{TH}	0.017	0.175	0.204	0.245	0.308
$T_{eq(calc)}$, ^{o}F	216	308	313	325	342
$T_{eq(meas)}$, ^{o}F	242	311	320	324	333

TABLE II. - COMPARISON OF REFLECTANCE $\overline{\rho}_a$ WITH THE QUANTITY $(1 - e_{TH})$

Aluminum					
Lab exposure, joules	0	1.25	2.68	5.6	25.4
$\overline{\rho}_a$ (for 420° K blackbody radiation)	1.01	0.80	0.76	0.62	0.305
$(1 - e_{TH})$	0.94	0.82	0.76	0.72	0.325
304 Stainless steel					
Lab exposure, joules	0	0.909	2.16	4.26	6.49
$\overline{\rho}_a$ (for 420° K blackbody radiation)	0.92	0.79	0.71	0.66	0.57
$(1 - e_{TH})$	0.89	0.78	0.70	0.66	0.63
Aluminum (1900 angstroms) on stainless steel					
Lab exposure, joules	0	1.05	1.98	4.51	6.08
$\overline{\rho}_a$ (for 420° K blackbody radiation)	1.02	0.81	0.77	0.67	0.63
$(1 - e_{TH})$	0.98	0.82	0.80	0.75	0.69

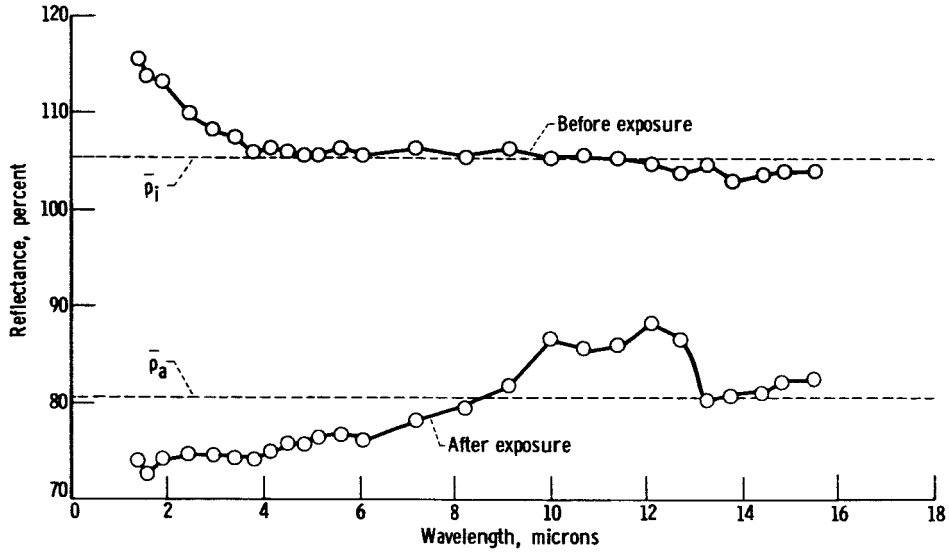

(a) Aluminum.

Figure 1. - Spectral reflectance ρ_{h-a} for polished metal surfaces exposed to approximately 1 joule of hypervelocity impaction.

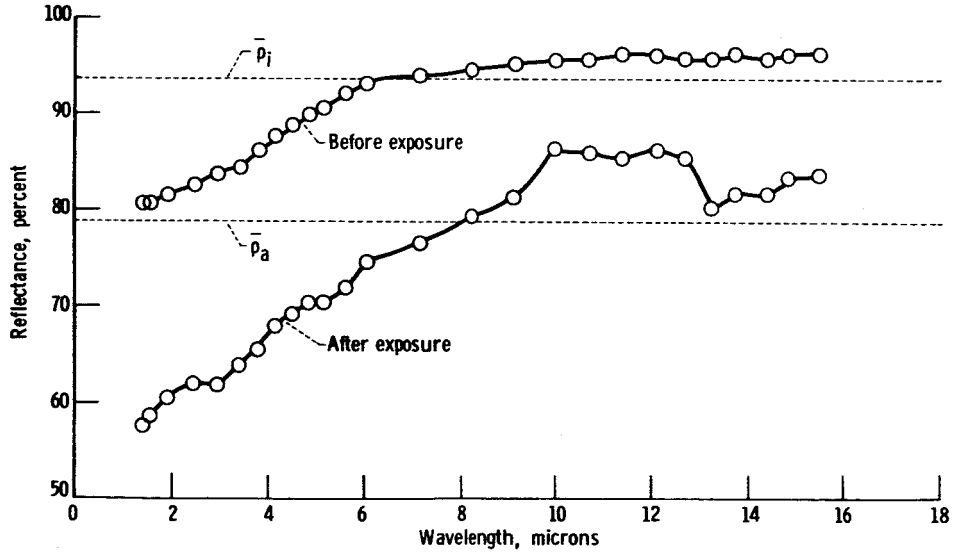

(b) Stainless steel 304.

Figure 1. - Continued. Spectral reflectance ρ_{h-a} for polished metal surfaces exposed to approximately 1 joule of hypervelocity impaction.

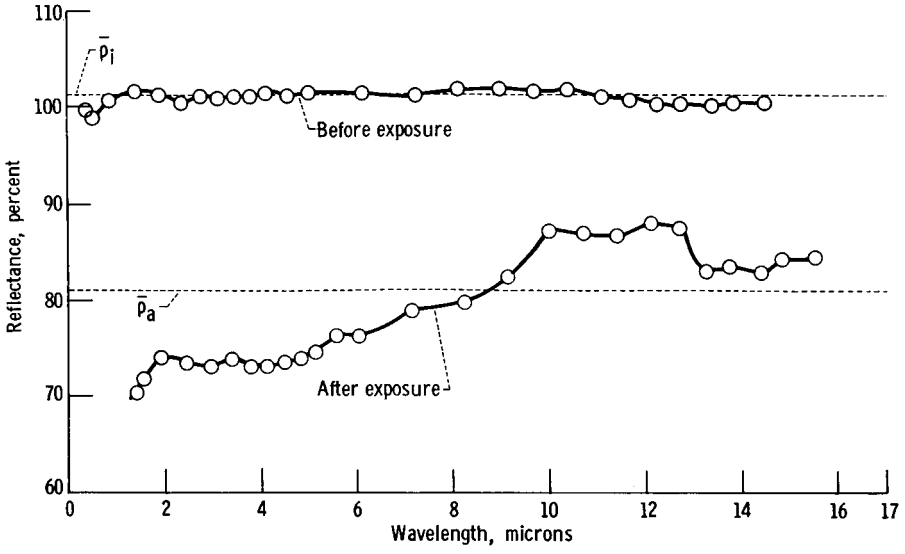

(c) 1900 Angstrom aluminum on stainless steel substrate.

Figure 1. - Concluded. Spectral reflectance ρ_{h-a} for polished metal surfaces exposed to approximately 1 joule of hypervelocity impaction.

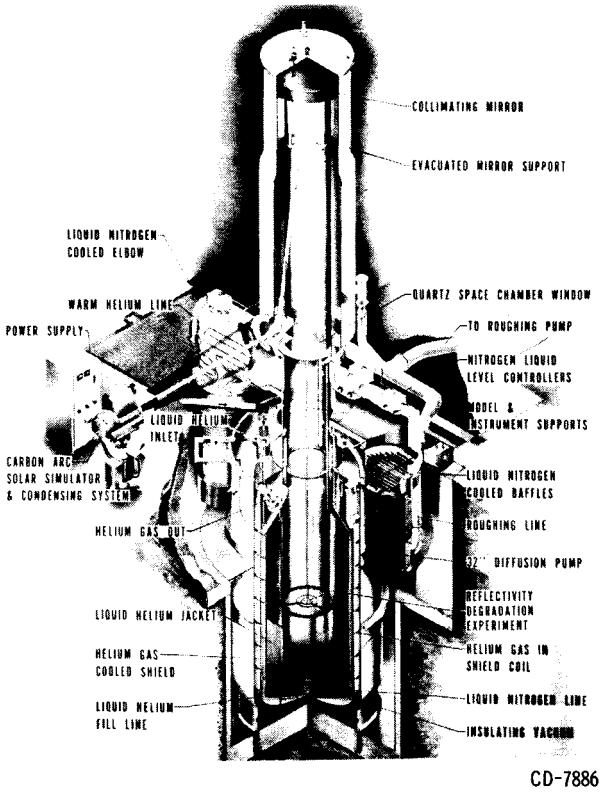

Figure 2. - Cutaway drawing of 10- by 6-foot solar space simulator.

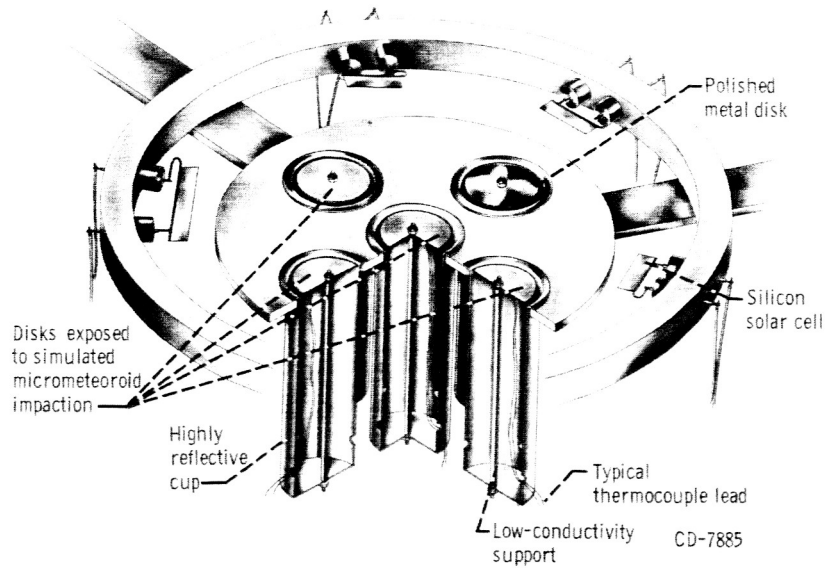

Figure 3. - Exposed metal disks in simulated satellite mounting.

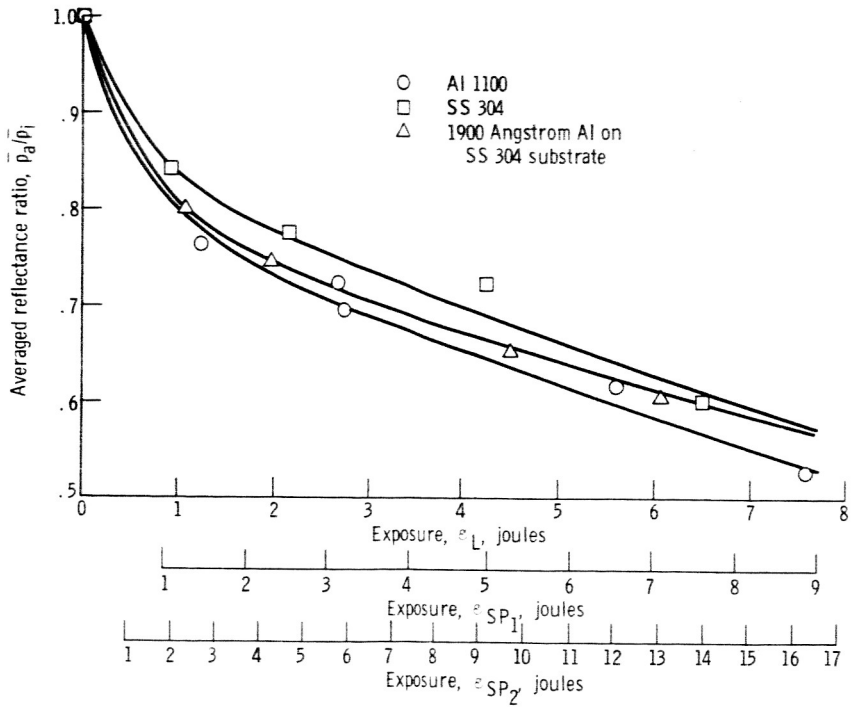

Figure 4. - Degradation of average reflectance of various metal surfaces after exposure to impaction by 6-micron SiC particles traveling at 8500 feet per second. (Extra abscissas added to indicate exposure necessary for equal damage in space. See appendix B.)

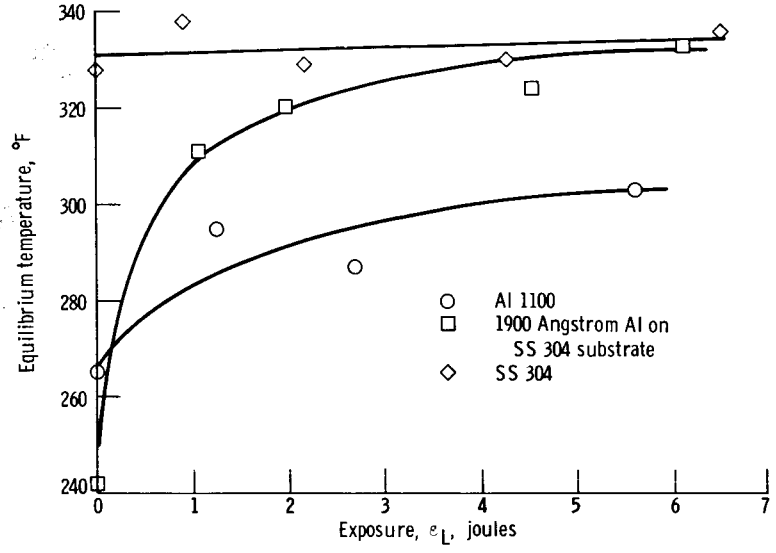

Figure 5. - Equilibrium temperature as function of surface exposure. Incident radiation, 1.25 solar constants.